

2-10-2006

Growth of Carbon Grains in Supernova Ejecta

Ethan A-N. Deneault
College of Charleston

Donald D. Clayton
Clemson University, claydonald@gmail.com

Bradley S. Meyer
Clemson University

Follow this and additional works at: https://tigerprints.clemson.edu/physastro_pubs

 Part of the [Astrophysics and Astronomy Commons](#)

Recommended Citation

Please use publisher's recommended citation.

This Article is brought to you for free and open access by the Physics and Astronomy at TigerPrints. It has been accepted for inclusion in Publications by an authorized administrator of TigerPrints. For more information, please contact kokeefe@clemson.edu.

GROWTH OF CARBON GRAINS IN SUPERNOVA EJECTA

ETHAN A.-N. DENEAULT

Department of Physics and Astronomy, College of Charleston, Charleston, SC 29422; deneaulte@cofc.edu

AND

DONALD D. CLAYTON AND BRADLEY S. MEYER

Department of Physics and Astronomy, Clemson University, Clemson, SC 29634; cdonald@clemson.edu, mbradle@clemson.edu

Received 2005 July 20; accepted 2005 October 8

ABSTRACT

We present a chemical reaction network that describes the condensation chemistry of carbon dust grains in an expanding supernova shell. We assume that the region of interest consists solely of gaseous free carbon and oxygen atoms and that the buildup of CO is counteracted by the radioactive decay of ^{56}Co , which breaks up the CO molecule and allows C to condense into solids. Our chemical model takes C to first form linear chains, which, at some critical length, transition into ringed isomers. These isomers are more resistant to oxidation than linear chains. These ringed isomers form the nuclei for the growth of larger carbon solids. The effect of the disruption of CO on grain growth is displayed, leading to a rethinking of previous assumptions on the importance of CO disruption. How the abundance and size distribution of grains are affected by various parameters of the ejecta is also studied, providing insight into the possible sites of grain condensation.

Subject headings: astrochemistry — infrared: stars — supernova remnants

1. INTRODUCTION

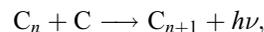
Presolar stardust grains are stellar condensates extracted from the matrix of unprocessed meteorites such as carbonaceous chondrites. The study of the isotopic composition of these grains has brought new understanding of the composition of Galactic stars that died before the Sun formed (Clayton & Nittler 2004). A small subclass (fewer than 1%) of presolar stardust grains exhibit peculiar isotopic anomalies, such as an overabundance of ^{44}Ca , daughter of the α -rich freezeout isotope ^{44}Ti , which point to these particular grains as being of supernova origin (Nittler et al. 1996; Hoppe et al. 1996). These isotopic anomalies are found uniformly throughout an individual stardust grain, implying that the grains must have condensed in a gas of that particular composition. Presupernova nucleosynthesis models (e.g., Woosley & Weaver 1995) indicate that probable regions for grain formation are near the core of the supernova, in an oxygen-rich environment. This can also be seen from the correlation between the $^{44}\text{Ti}/^{48}\text{Ti}$ and the $^{29,30}\text{Si}/^{28}\text{Si}$ ratios, consistent with condensation in these interior regions of the supernova. It is the goal of this study to understand the growth processes of graphite within the expanding supernova shell.

In the supernova interior, carbon chemistry progresses without the influence of hydrogen. Therefore, the chemistry is dominated by the reactions between carbon and oxygen. We follow Clayton et al. (1999, 2001; hereafter CLD99 and CDM01) in stressing the importance of the radioactivity on the subsequent chemistry of the cooling gas. In the absence of such supra-thermal radiation, a gas of C and O in chemical equilibrium will form nonreactive and tightly bound CO molecules. Gamma rays from the decay of ^{56}Ni and daughter ^{56}Co cascade through the ejecta, creating Compton electrons (Clayton & The 1991). Energizing collisions with these electrons have serious chemical consequences, notably the breakup of CO on a timescale of months. Because of this process, a kinetic chemistry model is favored.

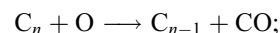
2. RATE EQUATIONS OF THE KINETIC MODEL

The chemical network proposed by CDM01 can be broken down into three sections: the growth of linear carbon chains, which is opposed primarily by oxidation; the isomerization of these linear chains into more oxidation-resistant ringed molecules; and the growth of carbon solids using these ringed isomers as nucleation sites. The steady state model developed by these authors relied on the chemical reaction timescale being much shorter than the timescale for large changes in the physical environment of the ejecta.

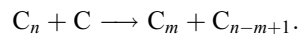
In this paper, we present a time-dependent kinetic network for the growth of carbon solids, beginning with linear chains and proceeding via isomerization to the growth of the grains themselves. Focusing solely on the essential components of carbon growth, we choose the ejecta to consist solely of monoisotopic ^{12}C and ^{16}O . The inclusion of less abundant species such as Si and Al adds only nonessential complexity to the growth process. We therefore take the primary chemical reactions for the growth of linear chains C_n to be (CDM01) radiative association of a carbon chain with a free C atom,



where $h\nu$ is a radiative quantum; oxidation of a larger chain to produce a CO molecule and a chain smaller by one C atom,



and C-induced “fission” of a large chain to produce two smaller chains,



In principle, chain-chain reactions can occur (Curl 1993); however, the contribution from these reactions appears to be insignificant. Each linear chain species C_n is characterized by its own

lifetime against isomerization, given by $\tau_{\text{iso}}(n)$, and a lifetime against thermal disruption, $\tau_{\text{th}}(n, t)$. In principle, nonthermal reactions, such as fast electrons, can disrupt linear chains. However, the lifetime against nonthermal disruption, typically months, is much longer than the thermal chemical reaction timescale, typically seconds. We therefore do not include nonthermal disruption of linear chains in the model. For small chains, $n < 10$, we assume that the lifetime against isomerization is effectively infinite. For chains of this length, it is not energetically preferable for the molecule to be in the ring isomer configuration (Weltner & Van Zee 1989), and therefore rings of this size will be exceedingly rare in the high-temperature ejecta. Chains with lengths longer than $n = 10$ may have isomerization lifetimes that are competitive with the chemical reaction timescale. The decrease in the temperature of the ejecta is proportional to the inverse of the time (e.g., Woosley et al. 2002), and we follow CDM01 in calculating $\tau_{\text{th}}(n, t)$ using detailed balance.

Previous works (CDM01) have hypothesized the idea of “population control” for grains: too many ringed isomers will lead to an overabundance of smaller grains, while too few will create very large, but exceedingly rare grains. Accurate knowledge of the production rates for ringed isomers requires that $\tau_{\text{iso}}(n)$ be known, or at the very least, be guessed appropriately. Unfortunately, these isomerization lifetimes are, at present, not known explicitly for any value of n . Large chains have many more vibrational modes than smaller chains. It is not surprising that longer chains tend to “flop around” and can wrap themselves into complex structures (Maruyama & Yamaguchi 1995). We therefore assume that the lifetime against isomerization decreases with increasing n based on this physical intuition alone.

In the steady state solution with “standard” rate coefficients (CDM01, their Table 1), the abundances of any chain pair C_{2n-1} and C_{2n} differ by a factor of about 2. However, the abundance of C_{2n+1} is 10^{-3} times that of the preceding species. The isomerization lifetime, $\tau_{\text{iso}}(n)$, must decrease by a factor of 1000 for every increase in n by 2 units if the isomerization of the lower abundance, larger chains is to produce more rings than the high-abundance chains just 2 units smaller. CDM01 also surveyed the sensitivity of the linear chain abundances to the values of the rate coefficients for even and odd chain lengths. If the association rate for even-length chains was increased by a factor of 10, for example, $\tau_{\text{iso}}(n)$ need only decrease by a factor of 100 for every 2 unit increase in n . In order to bypass these uncertainties, we define a *sole isomerizing species*, i.e., the chain length at which the rate of creation of ringed isomers $[N(C_n)\tau_{\text{iso}}(n)^{-1}]$ reaches its maximum value. The sole isomerizing species has index j , and the isomerization lifetime $\tau_{\text{iso}}(j)$ of the sole isomerizing species is a free parameter. In this paper we use only the “standard” rate coefficients of CDM01 for calculating the abundance of linear chains and refer interested readers to that work for a more detailed survey of chain growth.

After isomerization, the ringed molecules form nucleation sites for the growth of larger carbon solids. These isomers and the subsequent grains do not fission and are oxidized very slowly. We take the oxidation rate of grains, $k_{\text{O}}(n)$, to be 10^{-3} times the association rate $k_{\text{C}}(n)$ for free C and grains. Only when the free C abundance is less than one-thousandth of the O abundance does the oxidation of grains become important. Grains do not fission, and we do not include nonthermal disruption of grains. Thermal disruption of grains is a possibility when the temperature is above a few thousand K. However, when the temperature is above 2000 K, which we call the pre-grain-growth epoch, linear chains are disrupted very quickly by thermal effects, which drives the abundance of isomerizing species down. Only when

the temperature is below 2000 K do ringed isomers, and therefore grains, appear. We take the growth of carbon grains, therefore, to be wholly associative, except when the C/O ratio of the ejecta gas is extremely small. We write the set of reaction equations for carbon grains as simply the flow into the grain species G_n minus the flow out due to C association:

$$\begin{aligned} \frac{dG_n}{dt} &= N_{\text{C}}(t) \left[-k_{\text{C}}^g(j)G_j + \frac{N_j}{\tau_{\text{iso}}(j)} \right] \\ &= N_{\text{C}}(t) [-k_{\text{C}}^g(n)G_n + k_{\text{C}}^g(n-1)G_{n-1}], \end{aligned} \quad (1)$$

where $N_{\text{C}}(t)$ is the free carbon abundance at time t and the superscript g distinguishes grain reaction rates from linear chain reaction rates. As grains increase in size, they naturally will associate with carbon faster, due to their larger surface area. Therefore, we define the destruction rate of species n , $k_{\text{C}}^g(n)$, as proportional to the cross-sectional area of the grain and the association rate $k_{\text{C}}^g(j)$ for the first grain species,

$$k_{\text{C}}^g(n) = (n/j)^{2/3} k_{\text{C}}^g(j). \quad (2)$$

We take the association rate $k_{\text{C}}^g(j) = \langle \sigma_j^g v_T \rangle$ for the first grain species to be fast: $10^{-10} \text{ cm}^3 \text{ s}^{-1}$, which is the kinetic limit (CDM01).

Statistical evidence gathered from meteoritic data suggests that the radii of carbon stardust range from 0.1 to 20 μm (Clayton & Nittler 2004), with a mean of approximately 1 μm (approximately 10^{12} atoms). The network treats the growth of linear chains and grains atom by atom, so each grain that differs in size by a single atom is treated as a different species. Therefore, a mean-size grain of 10^{12} atoms requires the solution of 10^{12} simultaneous differential equations. To reduce the calculation of 10^{12} species to a more practical size, we grouped grains in bins of set width on a logarithmic scale, so that grain species $G_{101}-G_{200}$ constituted one bin, while $G_{201}-G_{300}$ and $G_{1001}-G_{2000}$ constituted two others, and so forth. Only species G_j through G_{50} were treated as separate species, and species $G_{51}-G_{100}$ comprise the first bin. We use the following notation when describing these binned species:

$$G_{a+1,b} = \sum_{i=a+1}^b G_i. \quad (3)$$

For any individual bin, the only important rates are the rate for input into the bin and the rate of flow out of the bin. To determine the latter, we recognize that equation (1) is similar to that of the s -process of neutron-capture nucleosynthesis in stars (Clayton et al. 1961). One of the features of the s -process is the *local approximation*; i.e., the ratio of abundances for two successive isotopes is inversely proportional to the ratio of neutron capture cross sections for those isotopes. This tends to minimize the difference in abundance between two successive species. In the s -process, the local approximation is only valid for isotopes between “magic” neutron numbers, where nuclear shells are filled. The growth of carbon grains has no such known restriction, and therefore we can assume the local approximation to be valid across any arbitrarily sized region in the capture chain. We take the local approximation to be valid within each bin individually, but not between bins, whose time-dependent relative abundances will be given by our calculations.

The outflow from any bin is always equal to the abundance of the last species in the bin times the association rate of that

species. We do not a priori know the abundance of the last species in any bin without knowing the individual abundances of every species in the bin. The total abundance of all species in the bin is known, however. We use the local approximation to determine an effective outflow rate such that the effective rate times the total abundance in the bin is exactly equal to the abundance of the last species times its own association rate:

$$\kappa_{a+1,b} = \left[\sum_{i=a+1}^b \frac{1}{k_C^g(i)} \right]^{-1}. \quad (4)$$

This effective rate follows from an assumption of the local approximation, namely, that $k_C(n)G_n$ is constant with n across the bin. The effective rate $\kappa_{a+1,b}$ is simply the reciprocal of the sum of the inverse rates from every species within the bin. If the bin only contains one species, it is trivial to show that $\kappa_{b,b}$ reduces to $k_C^g(b)$.

At early time, before any grain can have possibly grown to reach the last member in a bin, the outflow from that bin must necessarily be zero. However, using the effective rate (eq. [4]) for that bin, the outflow would begin as soon as that bin contains a nonzero abundance. Such rapid growth would be unphysical, because it ignores the time required for the grain to grow from the first member to the final member of the bin. Equation (4) assumes the local approximation to be established instantaneously, which is incorrect. Each reaction requires a mean time, defined as

$$dt_n = [N_C(t)k_C^g(t)]^{-1} = [N_C(t)(n/j)^{2/3} \langle \sigma_j^g v \rangle]^{-1}. \quad (5)$$

We therefore define a timelike variable called the fluence, the number of carbon atoms that impact a unit area in a time dt . The fluence τ is defined as

$$d\tau = N_C(t)v_T dt, \quad (6)$$

where v_T is the mean thermal velocity of the carbon atoms. Transforming equation (1) with the fluence and the effective rate, we find that it takes a simple form; the number of free carbon atoms is absorbed into $d\tau$. The new rate, κ' , differs from κ by a factor $1/v_T$, namely, $\kappa' = \kappa/v_T$, and

$$\frac{dG_{m+1,k}}{d\tau} = \left(-\kappa'_{m+1,k} G_{m+1,k} + \kappa'_{n+1,m} G_{n+1,m} \right). \quad (7)$$

Since we have defined the change in G in terms of the fluence of carbon atoms, we can determine the fluence required for a single carbon association, $d\tau_n = [(n/j)^{2/3} \kappa_j']^{-1}$ (this is equivalent to the statement in eq. [6]), and thus the total fluence needed to capture from the first grain species j to any species in the network,

$$\tau_{j \rightarrow n} = \tau_n = \frac{1}{\kappa_j'} \sum_{i=j}^n \left(\frac{j}{i} \right)^{2/3}. \quad (8)$$

Once the bins have been defined, the values of τ_n to arrive at the last member in each bin are constants. We can use the fluence to modify the grain growth equation (eq. [7]) in such a way that the output rate from the bin depends on the fluence that has oc-

curred within the model. In effect, maximal output from a bin will only be achieved as τ approaches τ_n , and

$$\frac{dG_{m+1,k}}{d\tau} = \left[-\kappa'_{m+1,k} T_k(\tau) G_{m+1,k} + \kappa'_{n+1,m} T_m(\tau) G_{n+1,m} \right]. \quad (9)$$

The rate $\kappa'_{n+1,m} T_m(\tau)$ is the fluence-corrected output rate for the bin $G_{n+1,m}$. It takes the values

$$\kappa'_{m,n} T_n(\tau) = \begin{cases} \kappa'_{m,n} \left(\frac{\tau}{\tau_n} \right)^b, & \tau < \tau_n, \\ \kappa'_{m,n}, & \tau \geq \tau_n. \end{cases} \quad (10)$$

We choose the parameter $b = 10$ as a ‘‘best fit’’ for all bins in the network. This choice is based on a number of numerical experiments that compare the abundance in a bin at time t to the sum of the abundances of each species in an exact solution, obtained from problems of smaller size. For example, the sum of the exact abundances of species $G_{51} - G_{100}$ can be compared to bin $G_{51,100}$ in our numerical scheme for various values of the parameter b . The same can be done for subsequent bins, as well. It is only when we expand the network beyond 10^3 species that the exact calculation becomes prohibitive. The correct value of b depends on the size of the bin; however, we have found that $b = 10$ performs remarkably well for all bin sizes that we calculated exactly.

3. FORMATION OF CO IN THE EJECTA

In the expanding and cooling supernova ejecta, free C and O will radiatively associate to form CO. Within the first year the less abundant of the two species would be bound in CO. CLD99 originally argued that the radioactive decay of ^{56}Ni and its daughter ^{56}Co provides a mechanism by which CO is disrupted, allowing for free C to exist in a region where the C/O ratio is less than unity. To test this assumption, we follow the chemical history of the ejecta when the temperature is much higher than 2000 K, which we define as the beginning of the grain growth epoch.

As shown by CDM01, linear carbon chains are thermally disrupted quickly if the temperature is much higher than 2000 K. CO, on the other hand, has a long lifetime against thermal disruption at temperatures near 4000 K. Detailed balance of the oxidation rate of free C shows the thermal lifetime of CO at 4000 K to be

$$\tau_{\text{th}}(\text{CO}, T) = \left(\frac{h^2}{2\pi m k T} \right)^{3/2} \frac{1}{k_{\text{O}}(\text{C})} e^{B(\text{CO})/kT},$$

$$\tau_{\text{th}}(\text{CO}, 4000 \text{ K}) \approx 7700 \text{ s}, \quad (11)$$

owing to the very high [$B(\text{CO}) = 11.09 \text{ eV}$] binding energy of the CO molecule. A long CO lifetime at high temperatures implies that in the pre-grain-growth epoch, the primary chemistry of the supernova is the oxidation of free carbon. In this high-temperature epoch, the formation of CO is countered by a higher radioactivity flux from the ^{56}Ni and ^{56}Co decay, but the rate of nonthermal destruction of CO is never fast enough to prevent at least some CO formation. At 10^7 s , we take the lifetime of CO versus nonthermal disruption to be $5 \times 10^6 \text{ s}$, but shorter at earlier times, owing to the exponential decrease of radioactivity over time.

If we assume homologous expansion, such that the density is inversely proportional to t^3 , and we take the temperature to be

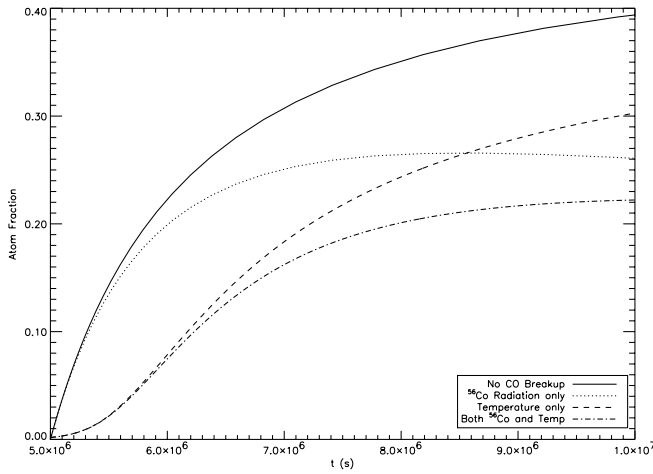


FIG. 1.—Total atom fraction of CO, comparing the effects of CO breakup via thermal and radiation effects. If CO is not disrupted (*solid line*), nearly 40% of the gas atoms are bound into CO, while thermal breakup and radioactivity (*dashed and dotted lines*) decrease the atom fraction of CO significantly. The bottom curve shows the CO atom fraction with both destruction channels operating.

inversely proportional to t (Woosley et al. 2002), we find that the temperature of the ejecta will reach 4000 K at approximately 5×10^6 s after core bounce and reach 2000 K at 10^7 s, the beginning of the grain growth epoch. One may wonder about the arbitrary choice of starting time for chemistry. If we begin the calculation earlier, say, 10^6 s (20,000 K), solutions given by the chemical network at 10^7 s are equal (to 1 part in 10^{10}) to the solutions if we had started the calculation at 5×10^6 s. On the other hand, if we start the chemical calculation later than 5×10^6 s, the abundances at 10^7 s are markedly smaller.

We set the initial conditions such that the density of the ejecta at 10^7 s is 10^{-13} g cm $^{-3}$ (Woosley et al. 2002). Because ρt^3 is a constant in homologous expansion, the bulk ejecta density is 8 times larger at 4000 K compared with 2000 K, so that the gaseous C and O atoms will interact more often.

How much CO is formed in the pre-grain-growth epoch? To consider this, we look at how the various destruction channels for CO (thermal and nonthermal) affect the abundance of CO at 10^7 s. Figure 1 plots the atom fraction of CO for different destruction channels for CO for an initial C/O ratio of 2/3. The atom fraction is defined to be the fraction of the total number of atoms in the network that are in a particular species. In the absence of radioactivity and with a gas temperature low enough such that $\tau_{\text{th}}(\text{CO})$ is very long, CO builds to an atom fraction of nearly 0.4 at 10^7 s. Destruction of CO by either thermal disruption or by radioactivity as plotted in Figure 1 reduces the atom fraction of CO at all times. Thermal disruption is the primary channel for CO breakup at early time, while the radioactivity-caused dissociation dominates through the mid and late pre-grain-growth epoch.

Figure 2, also with an initial C/O ratio of 2/3, compares different choices for the radioactive lifetime of CO at 10^7 s. The lifetime of CO at time t is inversely proportional to the amount of radioactivity present in the ejecta. If we remove the radioactivity flux from the model so that the CO lifetime versus non-thermal effects is effectively infinite (also shown in Fig. 1), the atom fraction of CO will reach nearly 30% of the total mass in the system by 10^7 s. If the lifetime of a CO molecule at 2000 K is on the order of 10^7 s, the CO atom fraction is nearer to 22% of the total at that time.

These findings do not completely support CDM01's assertion that in the absence of radioactivity, the less abundant of the

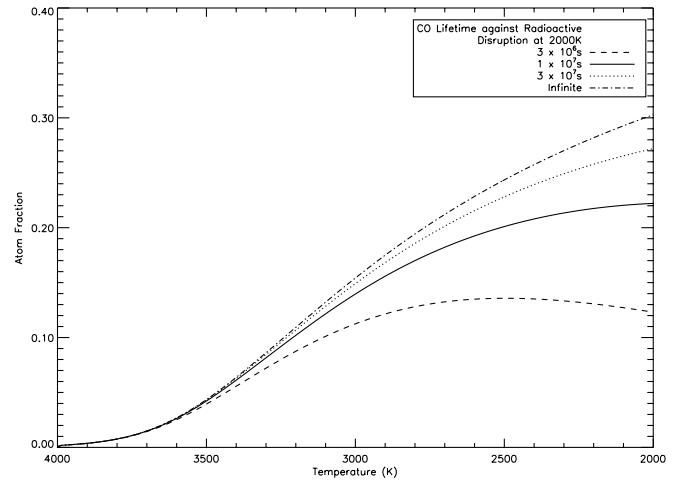


FIG. 2.—Total atom fraction of CO in the network as a function of temperature for different radioactive lifetimes of CO at 2000 K. If the lifetime of CO is infinite (no radiation), the atom fraction reaches 30% by 10^7 s. For shorter CO lifetimes (higher radioactivity flux), the atom fraction decreases.

two species will be bound completely in CO. Due to the effect of thermal radiation, even in a gas with C/O < 1, not all of the C is bound into CO in the pre-grain-growth epoch. This implies an abundance of free carbon in the gas regardless of radioactivity. Free C persists in the gas because the cross section for oxidation of the free carbon is small; not all free C can react in the time available. The density of the ejecta plays a very important role in the formation of CO. Figure 3 displays the percentage of C that is bound in CO as a function of the density of the system at the beginning of the grain growth epoch. Over 1 order of magnitude in the density, the percentage of C bound in CO increases significantly. The amount of CO created depends strongly on the density of the system. Differing model densities at 10^7 s in the grain-forming region can have significant consequences on the amount of free C available for grain growth.

4. CO IN SN 1987A

The supernova SN 1987A, which occurred in the Large Magellanic Cloud, was close enough for detailed study of the structure and chemistry of supernovae to be possible. By comparing

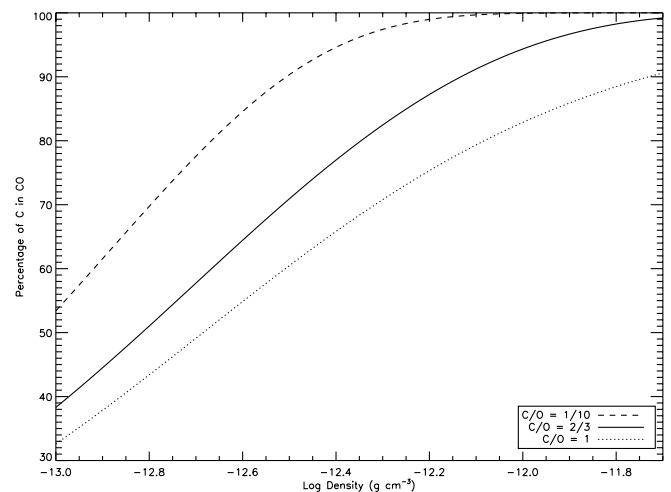


FIG. 3.—Percentage of carbon oxidized comparing different densities of the system at 10^7 s. These curves do not include thermal or nonthermal breakup of CO.

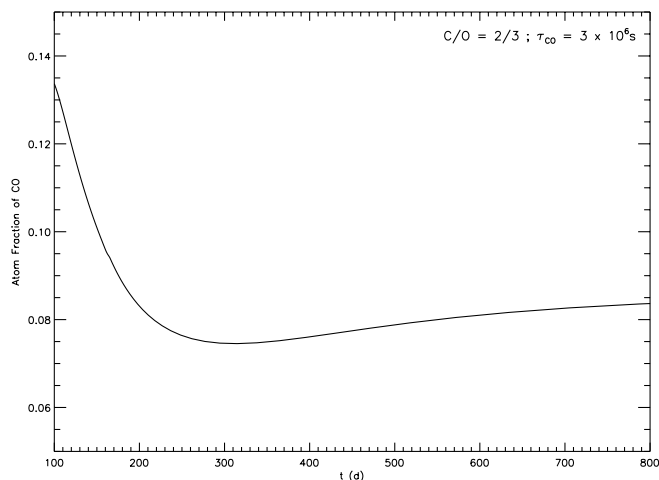


FIG. 4.—Total atom fraction of CO between 100 days after the explosion (8×10^6 s) and 800 days (7×10^7 s) for a C/O ratio of 2/3. Compare with Fig. 7 from Liu & Dalgarno (1995).

the observed line spectra of the supernova to thermochemical models (Liu et al. 1992) as well as dynamical models (Gearhart et al. 1999), it has been shown that the radioactivity has profound consequences on the formation of CO. We see this in our model quite clearly. The atom fraction of CO is greatly affected by the presence of the radioactivity (Fig. 1). The mass of CO as a function of time is described by Liu et al. (1992). The notable feature of their Figure 7 is the sharp decrease in the abundance of CO at early times, bottoming out near 300 days, and then slowly increasing. In Figure 4, using our model with a zone having a C/O ratio of 2/3 and a CO lifetime of 3×10^6 s, we find consistency with Liu et al. (1992), at least in the trend of the data.

Between 100 and 300 days in Figure 4, the atom fraction of CO decreases by a factor of 2, such that 8% of the total C and O atoms in the model are found in CO. This is much larger than the approximately 1%–2% that is observed in the spectra of SN 1987A. It is important to note, however, that this is a “one-zone” model. In actual supernovae, the bulk C/O ratio is not constant with radial mass coordinate, and a C/O ratio of 2/3 (in Fig. 4) is much higher than would be expected in the carbon shell of the ejecta (e.g., Gearhart et al. 1999, their Fig. 7). It is also not our goal to match our results directly with the spectra from one supernova, for that would limit the generality of our results. Our goal in this paper is to justify the conditions during the grain growth epoch.

5. GROWTH OF C GRAINS

In the ejecta, three primary parameters affect the growth of grains: the C/O ratio in the gas, the density of the gas at the beginning of the grain growth epoch, and the lifetime of CO against nonthermal breakup. Throughout this section, we use the linear chain C_{14} as the sole isomerizing species. This approximates the total rate of ring formation by the rate of isomerization of C_{14} . Moreover, we approximate the C_{14} abundance by the steady state abundance of C_{14} computed in the absence of isomerization. The choice is admittedly arbitrary.

In this section we plot the atom fraction versus species index for $G_j - G_{10^{15}}$. As described above, the grain species are binned in decades. The species index is simply a number that represents either a specific individual grain species or bin of many grain species. Table 1 shows the species index for selected bins. The characteristic “sawtooth”-like curve is not intended to represent a continuous solution; the bins represent discrete values and are

TABLE 1
SPECIES INDEX

<i>n, m</i>	Index	<i>n, m</i>	Index
14.....	20	$10^8 + 1, 2 \times 10^8$	112
15.....	21	$10^9 + 1, 2 \times 10^9$	121
16–50.....	22–56	$10^{10} + 1, 2 \times 10^{10}$	130
51, 100.....	57	$10^{11} + 1, 2 \times 10^{11}$	139
101, 200.....	58	$10^{12} + 1, 2 \times 10^{12}$	148
1001, 2000.....	67	$10^{13} + 1, 2 \times 10^{13}$	157
10001, 20000.....	76	$10^{14} + 1, 2 \times 10^{14}$	166
$10^5 + 1, 2 \times 10^5$	85	$10^{13} + 1, 2 \times 10^{13}$	157
$10^6 + 1, 2 \times 10^6$	94	10^{15}	175
$10^7 + 1, 2 \times 10^7$	103		

connected to guide the eye toward the trend in the data. Each “tooth” in the plot represents a set of bins in one decade; that is, the first “tooth” represents $G_{101,200} - G_{901,1000}$. Between each decade the number of species per bin increases by an order of magnitude, and thus the total atom fraction of those bins increases similarly. We use the term “maximum grain size” to refer to the bin with the highest atom fraction, or if there are many bins with a similar atom fraction, the bin with the largest particles. It is important to note that the “maximum” does not refer to the number of atoms in the grain. There are bins that contain more massive particles, but their atom fractions are significantly lower.

Throughout the ejecta, the C/O ratio is not constant (Woosley et al. 2002). In the dense interior C-O core, the C/O ratio is very small, $\sim 10^{-1}$, while in the C-rich He shell, the ratio is greater than unity. Figure 5 plots the computed atom fraction of grain species for selected values of the bulk C/O ratio. As expected, a bulk C/O ratio near unity provides enough free carbon for the largest grains (10^{12} to 10^{13} atoms) to contain a high fraction of the total carbon in the system. If the bulk C/O ratio is less than unity, carbon grains still condense, but with a reduced atom fraction, indicating a lower abundance per species. With a low bulk ratio, smaller grains have a much higher atom fraction than the largest grains, as well.

The lifetime of CO has a marked effect on how much CO grows in the pre-grain-growth epoch. In Figure 2, for a density of 10^{-13} g cm^{-3} at 10^7 s and C/O = 1, a short CO lifetime of about a month (2×10^6 s) reduces the abundance of CO at 10^7 s

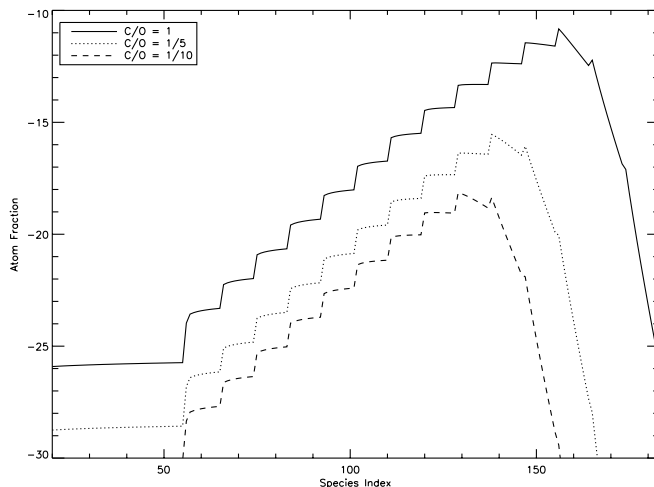


FIG. 5.—Atom fraction of grain species at 10^8 s, comparing different C/O ratios, for $j = 14$. (See Table 1 for tabulated species index.)

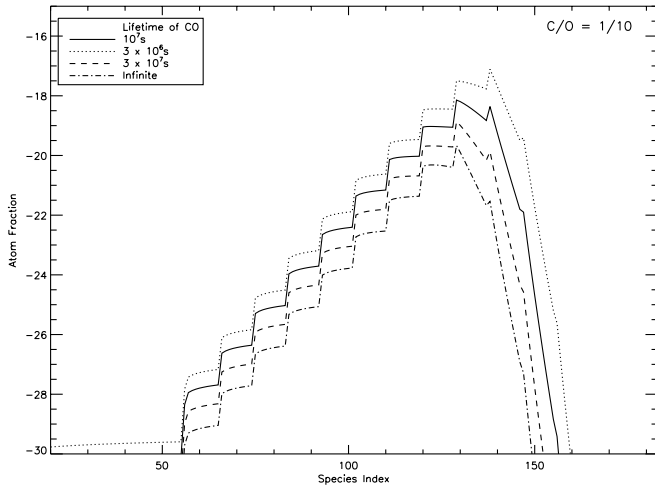


FIG. 6.—Atom fraction of grain species at 10^8 s with a C/O ratio of 1/10, comparing various CO lifetimes, for $j = 14$. (See Table 1 for tabulated species index.)

by about 18%. With those values for the ejecta density and CO lifetime, even in the absence of radioactivity, the atom fraction of CO is not above 0.3 before 10^7 s. Free C and O gas is available at the beginning of the grain growth epoch. The atom fraction of large carbon grains is not significantly affected by the lifetime of CO when the C/O ratio is near unity.

For smaller bulk C/O ratios, the CO lifetime has a greater effect on the atom fraction of grain species: gas with a C/O ratio much less than unity will trap a larger fraction of the free C gas into CO during the pre-grain-growth epoch. Figure 6 compares the atom fraction of the grain species and bins at 10^8 s for a C/O ratio of 1/10 with a “low” density $\rho(10^7$ s) of 10^{-13} g cm^{-3} . The atom fraction of the grain species decreases, as expected, with longer CO lifetimes, and the maximum grain size is reduced: 10^{11} atoms (species index 139) at a CO lifetime of 3×10^6 s and 10^{10} atoms (species index 130) at an infinite (no radioactivity) CO lifetime. The bin atom fractions differ by less than an order of magnitude between an infinite CO lifetime and a CO lifetime of 3×10^7 s. Shorter CO lifetimes, representing a greater radioactivity flux, produce more grains of every size. However, a CO lifetime of roughly a month (3×10^6 s) shows only a factor of 100 increase in the atom fraction for all but the largest grain sizes. The choice of the “low” density here is critical for these results. In this “low” density ejecta, most, but not all of the free C gas has been trapped into CO in the pre-grain-growth epoch. Since free C is available, grains will grow regardless of whether CO is disrupted or not. If the density at 10^7 s is higher by 1 order of magnitude, $\rho(10^7$ s) = 10^{-12} g cm^{-3} , the radioactive breakup of CO becomes the primary driver of grain formation.

In Figure 7 we display the atom fraction of grains for the same C/O ratio, but with this higher density. Without the ^{56}Co radioactivity to break up CO, grain growth is negligible; the highest atom fraction of any grain bin without CO disruption is 10^{-58} , and the maximum grain size is 10^5 atoms (species index 85). A small radioactivity flux from ^{56}Co , such that the CO lifetime is one year (3×10^7 s), produces a staggering change in the atom fraction of the grain species and bins of nearly 20 orders of magnitude. Grains created with this CO lifetime have an atom fraction of 10^{-33} at the maximum grain size of 10^{10} atoms (species index 130). The atom fraction is still very small, but the breakup of CO allows for even this limited grain growth. For shorter CO lifetime, the abundance of grains increases, as does the maximum size of the grains. Also shown on Figure 7 is the

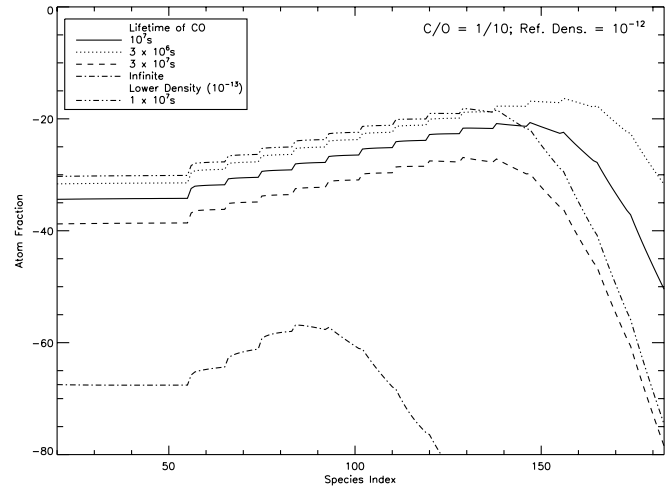


FIG. 7.—Atom fraction of grain species at 10^8 s with a C/O ratio of 1/10 and a reference density of 10^{-12} , comparing various CO lifetimes, for $j = 14$. (See Table 1 for tabulated species index.)

atom fraction of grains with a CO lifetime of 10^7 s from Figure 6. If we compare the curves at that CO lifetime between the low-density calculation and the higher density calculation, we find that the higher density calculation produces more high-mass grains than the lower density calculation. High-density ejecta produces larger grains, because there is more time for grain growth before the density becomes too low to sustain chemistry. In the absence of radioactivity, lower density regions create more grains than higher density regions, because CO does not trap all of the free C before the grain growth epoch. In high-density regions, CO is an effective carbon trap, and the absence of radioactivity prohibits grain growth.

Observations of SN 1987A confirm that supernovae do condense dust, and subsequent theoretical studies have attributed a large fraction of the dust in the interstellar medium (ISM) to Type II supernovae (e.g., Dunne et al. 2003). Within the first year after SN 1987A, a nonblackbody infrared spectrum was observed in the ejecta, leading to the inference of condensing dust in the inner regions of the supernova beginning near 350 days, and speeding up near 500 days (McCray 1993). This timescale is similar to our model, as we confine dust growth to temperatures below 2000 K (10^7 s), and the largest grains do not grow until nearly $(3-4) \times 10^7$ s. SN 1987A is estimated to have ejected $3 \times 10^{-4} M_{\odot}$ of dust of various compositions (graphite, SiC, Fe_3O_4 , etc.; McCray 1993) to account for the infrared emission observed. However, this amount may only be a lower limit to the actual dust produced within the ejecta; theoretical models show that possibly up to $1 M_{\odot}$ of dust could be produced in a $20 M_{\odot}$ supernova, such as SN 1987A (Dwek 1988). The model presented in this dissertation does produce graphite dust. Depending on the physical parameters of the ejecta and the sole isomerizing species, very large grains of $\approx 10^{13}$ atoms have atom fractions near 10^{-5} ; 1 atom out of every 10^5 belongs to a grain near this size. Although we cannot directly compare the atom fraction of grains created by our model to the ejected mass of dust from SN 1987A, it is clear that a significant fraction of carbon can be found in dust condensed inside the ejecta.

6. SUMMARY

We have provided a time-dependent kinetic chemistry model for the condensation of carbon gas in a cooling and homologously expanding Type II supernova ejecta. The interaction of the ejecta with gamma rays created from the decay of ^{56}Ni and ^{56}Co creates

TABLE 2
SELECTED SENSITIVITIES OF GRAIN ABUNDANCES IN THE PARAMETER SPACE $\{C/O, \tau_{CO}(t_{ref}), \rho(t_{ref})\}$

C/O	$\tau_{CO}(10^7 \text{ s})$	$\rho(10^7 \text{ s})$	Grain Size	Atom Fraction
>1	Short ^a	High ^b	Maximally large (10^{14+})	Very high (10^{-5+})
$\ll 1$	Short	High	Very large ($10^{12-10^{13}}$)	Low (10^{-20})
$\ll 1$	Long ^c	Low ^d	Midrange (10^9)	Low
<1	Infinite	Low	Midrange	Low
<1	Infinite	High	Extremely small (10^4)	Negligible (10^{-60})

^a $\tau_{CO}(10^7 \text{ s}) = 2 \times 10^6 \text{ s}$.

^b $\rho(10^7 \text{ s}) = 1 \times 10^{-12} \text{ g cm}^{-3}$.

^c $\tau_{CO}(10^7 \text{ s}) = 3 \times 10^7 \text{ s}$.

^d $\rho(10^7 \text{ s}) = 1 \times 10^{-13} \text{ g cm}^{-3}$.

Compton electrons. This provides a nonthermal destruction channel for the otherwise nonreactive CO molecule. Depending on the density and C/O ratio of the gas, anywhere from 15% to 100% of the free carbon atoms in the supernova are oxidized to CO before the temperature of the ejecta drops to 2000 K, which begins the epoch of grain growth. Three parameters characterize the growth of carbon solids in the cooling ejecta: the bulk C/O ratio, the lifetime of the CO molecule against nonthermal disruption [$\tau_{CO}(t)$], and the density of the ejecta $\rho(t)$. Table 2 shows the resulting grain growth for selected values of these three parameters.

The density of the ejecta plays an important role in the growth of carbon solids. In a lower density ejecta, CO does not form an effective trap for carbon in the pre-grain-growth epoch. This allows for grains to condense regardless of the presence of radioactivity. In ejecta that is of higher density, the nonthermal disruption of CO by radioactivity is essential for the growth of grains. That the breakup of CO is not *required* for grain formation in a low-density region is a new and unexpected result that would not be possible in statistical equilibrium. We emphasize once again that application of thermal equilibrium to supernova ejecta gives a very poor approximation for the problem of carbon dust. By analyzing the controlling kinetic factors, we have

shown that a kinetic approach along the lines of this work is necessary to model the growth of carbon dust. We have also shown that distinct zones of differing C/O ratio and differing density will give markedly different results for grain growth. More realistic results require the supernova to be modeled zone by zone.

Thus far, we have not addressed the survival of these grains during the reverse shocks that the material zones encounter. Deneault et al. (2003) discussed many aspects of these reverse shocks for the new dust and noted especially that sputtering by oxygen atoms and thermal evaporation may present serious obstacles to their survival. These destructive processes must also be taken into account in realistic models of supernova grain growth and survival.

This research is supported by the National Aeronautics and Space Administration under grants NAG5-10454 and NAG5-11871 issued through the Office of Space Science and by DOE grant DE-FC02-01ER41189. The authors would also like to thank Alex Heger for the use of his $25 M_{\odot}$ model supernova data.

REFERENCES

- Clayton, D. D., Deneault, E. A.-N., & Meyer, B. S. 2001, ApJ, 562, 480 (CDM01)
- Clayton, D. D., Fowler, W. A., Hull, T. E., & Zimmerman, B. A. 1961, Ann. Phys., 12, 331
- Clayton, D. D., Liu, W., & Dalgarno, A. 1999, Science, 283, 1290 (CLD99)
- Clayton, D. D., & Nittler, L. R. 2004, in Origin and Evolution of the Elements, ed. A. McWilliam & M. Rauch (Cambridge: Cambridge Univ. Press), 300
- Clayton, D. D., & The, L. 1991, ApJ, 375, 221
- Curl, R. F. 1993, Philos. Trans. R. Soc. London A, 343, 19
- Deneault, E. A.-N., Clayton, D. D., & Heger, A. 2003, ApJ, 594, 312
- Dunne, L., Eales, S., Ivison, R., Morgan, H., & Edmunds, M. 2003, Nature, 424, 285
- Dwek, E. 1988, ApJ, 329, 814
- Gearhart, R. A., Wheeler, J. C., & Swartz, D. A. 1999, ApJ, 510, 944
- Hoppe, P., Strebels, R., Eberhardt, P., Amari, S., & Lewis, R. S. 1996, Science, 272, 1314
- Liu, W., & Dalgarno, A. 1995, ApJ, 454, 472
- Liu, W., Dalgarno, A., & Lepp, S. 1992, ApJ, 396, 679
- Maruyama, S., & Yamaguchi, Y. 1995, Thermal Sci. Eng., 3, 105
- McCray, R. 1993, ARA&A, 31, 175
- Nittler, L. R., Amari, S., Zinner, E., Woosley, S. E., & Lewis, R. S. 1996, ApJ, 462, L31
- Weltner, W., & Van Zee, R. J. 1989, Chem. Rev., 89, 1713
- Woosley, S. E., Heger, A., & Weaver, T. A. 2002, Rev. Mod. Phys., 74, 1015
- Woosley, S. E., & Weaver, T. A. 1995, ApJS, 101, 181